25th Summer School and International Symposium on the Physics of Ionized Gases—SPIG 2010 IOP Publishing
Journal of Physics: Conference Series **257** (2010) 012011 doi:10.1088/1742-6596/257/1/012011

Interactions of ions with graphene

I Radović[1], N Bibić[1] and Z L Mišković[2]

[1]VINČA Institute of Nuclear Sciences, University of Belgrade, P.O. Box 522, 11001, Belgrade, Serbia

[2]Department of Applied Mathematics, University of Waterloo, Waterloo, Ontario, Canada N2L 3G1

E-mail: iradovic@vin.bg.ac.rs

Abstract. We evaluate the stopping and image forces on a charged particle moving parallel to a single sheet of graphene supported by an insulating substrate under the gating conditions. The forces are presented as functions of the particle speed and the particle distance for a broad range of charge-carrier densities in graphene. We also consider the effects of a finite gap between graphene and a supporting substrate, as well as the effects of a finite damping rate that is included through the use of Mermin's procedure. The damping rate is estimated from a tentative comparison of the Mermin loss function with a high-resolution reflection electron energy loss spectroscopy experiment.

1. Introduction

Graphene is a flat monolayer of carbon atoms tightly packed into a two-dimensional (2D) honeycomb lattice [1]. It is a basic building block for graphitic materials of all other dimensionalities: highly oriented pyrolytic graphite (HOPG, a stack of graphene layers), carbon nanotubes (rolled-up cylinders of graphene) and fullerene molecules (consisting of wrapped graphene by the introduction of pentagons on the hexagonal lattice) [2, 3]. Interactions of fast-moving charged particles with various carbon nanostructures have been investigated in recent years, e.g., in the electron energy loss spectroscopy (EELS) of carbon nanotubes [4] and isolated layers of free-standing graphene [5].

On the other hand, interactions of energetic heavy charged particles with graphene-based materials have been studied extensively for some time, e.g., in investigations of the directional effects in ion and molecule implantation into HOPG [6, 7], ion channelling through HOPG [8] and secondary electron emission from HOPG induced by fast ions [9] and clusters [10], as well as in ion channelling through carbon nanotubes [11, 12, 13, 14].

In order to better understand particle interactions with layered graphitic nanostructures and motivated by these developments, we explore here the effects of dynamic polarization of graphene on forces acting on ions moving parallel to it. Specifically, we calculate the dissipative force which opposes the ion's motion, called the stopping force, and the perpendicularly oriented conservative force which bends the ion's trajectory towards the sheet, called the image force.

Generally speaking, the easiest way to calculate these forces is based on a 2D hydrodynamic model [15] which proved itself to be a valuable theoretical tool for qualitative understanding of the high-frequency, collective excitations in carbon nanotubes [11, 16]. In the previous publications we have used a simpler, one-fluid hydrodynamic model, which treats all four carbon's valence electrons as a

single fluid, to evaluate the dynamic image force on protons channelled through carbon nanotubes in the MeV energy range [13, 17, 18], as well as the stopping and image forces on fast ions moving parallel to a single sheet of graphene supported by an insulating substrate [19] and the stopping and image forces up to the second order on fast ions moving parallel to free-standing graphene [20]. We have also calculated, in the previous publications, the stopping and image forces on projectiles moving parallel to both carbon nanotubes [11, 12] and supported graphene [21] using the linearized two-fluid hydrodynamic model, which makes distinction between the contributions of carbon's σ and π electrons to plasmon excitations in these structures. We have also used the two-fluid hydrodynamic model to study the wake effect in interactions of fast ions with supported graphene [22].

In order to evaluate the stopping and image forces on slow ions moving parallel to a supported graphene under the gating conditions, the dielectric-response theory for surfaces and layered structures [23] is a convenient way to proceed, given that the dielectric function for graphene is available within the random phase approximation (RPA) based on a linear approximation for the π electron bands [24, 25, 26]. We also use a kinetic (Vlasov) equation approach which yields a relatively simple dielectric function that describes both the intraband single-particle excitations (SPEs) and plasmon excitations in graphene's π bands within the linearized electron energy dispersion approximation [27, 28].

Graphene usually appears in experimental situations as supported by a substrate [29, 30]. While the configuration of graphene on metal [29] opens interesting possibility of exciting novel modes of collective electron excitations due to plasmon hybridization [12, 31], we limit ourselves here to the insulating substrate, such as SiO_2 lying underneath a single graphene sheet [30]. Surprisingly, while Ishigami *et al.* [30] have found that the distance h between graphene and substrate is on the order of the distance between graphene layers in graphite or even larger, all theoretical models of graphene's dynamic response assume a zero gap between the graphene and a substrate [24, 25]. One of our principal goals is to demonstrate just how strong are the effects of finite h in the dynamic-polarization forces on moving ions, implying a need to include the gap size explicitly in modelling of other screening phenomena by graphene.

Although we consider the RPA dielectric function to be a basic, parameter-free model that provides an adequate description of both the interband and intraband SPEs, as well as plasmon excitations, in graphene, the model nevertheless has its shortcomings. For example, it ignores the local-field effects (LFE) due to electron-electron correlations [4, 32] and assigns an infinitely long lifetime to the electron excitations. The latter deficiency is often rectified in *ab initio* studies by applying a finite broadening, on the order of $0.5\,eV$, to the frequency domain for calculations of the loss function [5]. In a similar way, one can introduce a finite relaxation time, or decay (damping) rate, γ, to the RPA dielectric function for graphene using Mermin's procedure [33, 34]. Since there are many scattering processes that can give rise to a finite lifetime of the excited π electrons in graphene, an accurate determination of γ still presents a challenge [34, 35]. Therefore, we make one of our principal goals to estimate γ by comparing the RPA model with finite damping to the experimental data for the high-resolution reflection EELS (HREELS) spectra of graphene on a SiC substrate [36].

The parameters of primary interest in this study are the equilibrium density of charge carriers in graphene, n, the graphene-substrate gap height, h, and the damping rate, γ. The equilibrium density is particularly important because it determines the Fermi momentum of graphene's π-electron band, $k_F = \sqrt{\pi n}$, and the corresponding Fermi energy, $E_F = \hbar k_F v_F$, where $v_F \approx c/300$ is the Fermi speed of the linearized π band and c is the speed of light in free space. In this paper, we consider a wide range of densities $n \geq 0$, expressed as a multiple of the base value $n_0 = 10^{11}\,cm^{-2}$. Note that we use Gaussian electrostatic units.

2. Forces on moving charges

We use a Cartesian coordinate system with coordinates $\{\vec{R}, z\}$ and assume that graphene is located in the plane $z = 0$, where $\vec{R} = \{x, y\}$ is position in the plane and z distance from it. A substrate with dielectric constant ε_s is assumed to occupy the region $z \le -h$ underneath the graphene, whereas the region $z > -h$ is assumed to be vacuum or air. It can be shown that, for a point charge Ze moving parallel to graphene with speed v at a fixed distance $z_0 > 0$, the stopping and image forces are given by, respectively

$$F_s = \frac{2Z^2e^2}{\pi v}\int_0^\infty e^{-2qz_0}dq\int_0^{qv}\frac{\omega}{\sqrt{q^2v^2-\omega^2}}\,\mathrm{Im}\left[\frac{1}{\varepsilon(q,\omega)}\right]d\omega, \tag{1}$$

$$F_i = \frac{2Z^2e^2}{\pi}\int_0^\infty qe^{-2qz_0}dq\int_0^{qv}\frac{1}{\sqrt{q^2v^2-\omega^2}}\,\mathrm{Re}\left[\frac{1}{\varepsilon(q,\omega)}-1\right]d\omega, \tag{2}$$

where we have used the symmetry properties of the real and imaginary parts of the dielectric function of supported graphene

$$\varepsilon(q,\omega) = \varepsilon_0(q) + \frac{2\pi e^2}{q}\chi(q,\omega), \tag{3}$$

with $\chi(q,\omega)$ being the polarization function for free graphene and

$$\varepsilon_0(q) \equiv \frac{1}{1-\frac{\varepsilon_s-1}{\varepsilon_s+1}e^{-2qh}}, \tag{4}$$

is the background dielectric function which quantifies the effects of substrate on the response of graphene. Note that $\varepsilon_0(q)$ takes the values in the range between 1 and $(\varepsilon_s+1)/2$, characterizing, respectively, the case of a free-standing graphene ($h \to \infty$) and the case of a zero gap ($h = 0$) between graphene and a substrate.

We first present the stopping and image forces calculated with dielectric functions from the kinetic equation (KE) model [27] and the random phase approximation (RPA) model [24, 25, 37] for free graphene ($h \to \infty$) and a vanishing damping rate ($\gamma \to 0$). The results for both forces are normalized by $F_0 = Z^2e^2/(4z_0^2)$, the magnitude of the classical image force on a static point charge a distance z_0 from a perfect conductor, to better reveal differences between the two models.

The difference between the KE and RPA models at low particle speeds ($v < v_F$) is analyzed in figure 1. We compare the normalized stopping and image forces on a proton ($Z = 1$) moving at a speed $v = v_F/2$ above free graphene as a function of the particle distance z_0, for a broad range of densities. At such low speeds, one can see that the agreement between the KE and RPA models is better for the image force than it is for the stopping force. It follows from figure 1 that the condition $z_0k_F > 1$ may suffice as a rough criterion for the application of the KE model at low speeds. This condition is far less restrictive than $z_0k_F >> 1$, which is required for the application of the KE model at high speeds ($v > v_F$).

We now use the RPA dielectric function with a vanishing damping rate ($\gamma \to 0$) to evaluate the stopping and image forces, and investigate the effects of a finite graphene-substrate gap. We assume that graphene is supported by a SiO_2 substrate ($\varepsilon_s \approx 3.9$) and consider the gap heights $h = 0$ for the zero gap commonly considered in the literature, $h = 4$ Å for a realistic value [30] and $h \to \infty$ for free graphene.

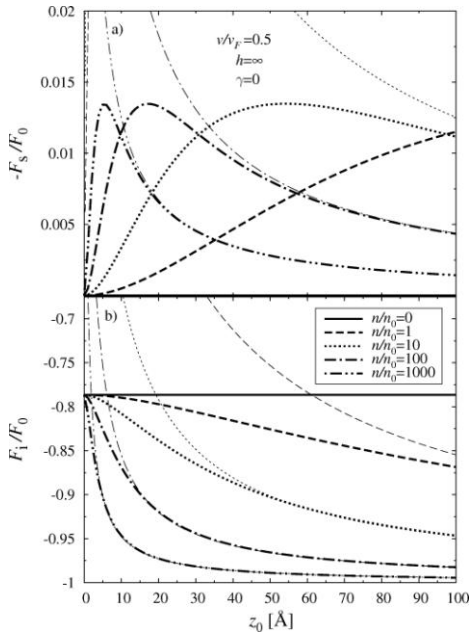

Figure 1. The stopping force (a) and image force (b) normalized by $F_0 = Z^2 e^2 / (4z_0^2)$ and shown as a function of the distance z_0 of a proton ($Z = 1$) moving at a reduced speed $v/v_F = 0.5$ above free graphene ($h \to \infty$) for several values of the reduced charge-carrier density n/n_0, where $n_0 = 10^{11}\, cm^{-2}$. The thick and thin lines represent the results from the RPA and KE models with vanishing damping ($\gamma \to 0$), respectively.

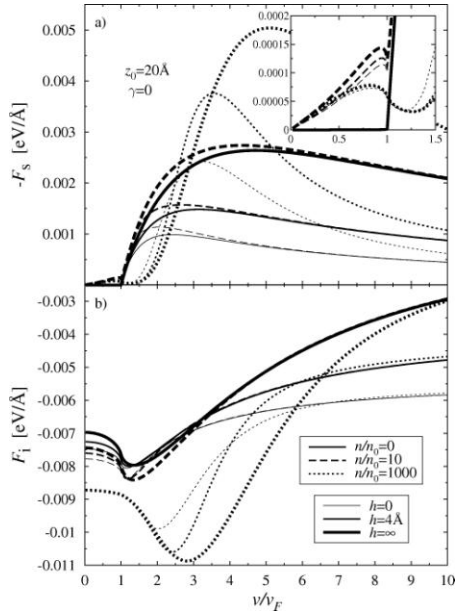

Figure 2. The stopping force (a) and image force (b) from the RPA model with vanishing damping ($\gamma \to 0$) shown as a function of the reduced speed v/v_F of a proton ($Z = 1$) moving at a distance $z_0 = 20$ Å above graphene on a SiO_2 substrate ($\varepsilon_s \approx 3.9$). Results are shown for several values of the gap height h and several values of the reduced charge-carrier density n/n_0, where $n_0 = 10^{11}\, cm^{-2}$.

In figure 2, we compare the velocity dependence of the stopping and image forces on a proton moving at a distance $z_0 = 20$ Å above graphene for several gap heights and densities. For low particle speeds ($v < v_F$), the gap height has a relatively small influence on the stopping and image forces that diminishes as the charge-carrier density increases and effectively screens out the graphene-substrate gap. The density n is therefore the most important parameter in the low-speed behavior of both forces. For higher particle speeds, the charge carriers in graphene are not as effective in screening out the graphene-substrate gap, and hence the gap height has a much stronger effect on the stopping and image forces. In particular, figure 2 shows that for sufficiently high speeds ($v >> v_F$) an increase in the gap height tends to increase the strength of the stopping force and decrease the strength of the image force, but there is a range of moderate speeds for which this trend is reversed. One may conclude that in the RPA model, as in the KE model [27], any uncertainty or local variations in the gap height across graphene can lead to large fluctuations in the stopping and image forces, particularly for high particle speeds.

3. Comparison with HREELS experiment

In this section, we use the RPA model with a finite damping rate $\gamma > 0$ by means of the Mermin dielectric function $\varepsilon_M(q,\omega,\gamma)$ (see appendix in reference [37]). To obtain a reasonable estimate for γ, we compare the RPA model with finite damping to the experimental data for the HREELS spectra of graphene on a SiC substrate [36].

In figure 3, we display a tentative comparison between the HREELS data [36] and the Mermin loss function $\mathrm{Im}[-1/\varepsilon_M(q,\omega,\gamma)]$ with $\hbar\gamma = 0$, 200, and $400\ meV$ and a gap height of 1Å for wavenumbers ranging from 0.008 to 0.102 Å^{-1}. The SiC substrate is treated in the static mode with dielectric constant $\varepsilon_s = 9.7$, and the equilibrium density in graphene is set at $n = 2\cdot 10^{13}\ cm^{-2}$ (hence $E_F \approx 570\ meV$ and $k_F \approx 0.08$ Å^{-1}) to match experimental conditions. Note that since the HREELS data is scaled arbitrarily, the Mermin loss functions for $\hbar\gamma = 200$ and $400\ meV$ are scaled so that the maximum peak heights coincide with those from the experiment. For $\hbar\gamma = 0$, however, the singular plasmon peak prevents such a scaling, and so the Mermin loss function is scaled by the same factor as for the $\hbar\gamma = 400\ meV$ loss function.

In figure 3, the range $q \le k_F$ is particularly interesting because the Mermin loss function with $\hbar\gamma = 0$ exhibits three distinct features for these wavenumbers: a continuous spectrum of intraband SPEs for $0 < \omega < qv_F$, a continuous spectrum of interband SPEs for $\omega > v_F(2k_F - q)$, and a narrow plasmon line at $\omega = \omega_p(q)$ in the otherwise void interval $qv_F < \omega < v_F(2k_F - q)$. The fact that these three features are not visible in the experimental HREELS spectra can be tentatively explained by assuming that a large enough damping rate γ exists, due to various scattering mechanisms, that a broadened plasmon line merges into the two regions of SPEs to form a single peak that follows approximately the original plasmon dispersion curve, $\omega = \omega_p(q)$. Note that a broadening of the plasmon line for the $\hbar\gamma = 0$ loss function does occur for the wavenumbers $q = 0.077$ and 0.102 Å^{-1} as the plasmon line crosses the boundary $\omega = v_F(2k_F - q)$ and enters into the region of interband SPEs, in which collective plasma oscillations decay into SPEs in a way that can be described by a finite Landau damping rate, γ_L [38]. For the Mermin loss function with a phenomenological damping rate γ, however, a broadening of the plasmon line occurs for all q. Figure 3 shows that a reasonably good qualitative agreement with the experiment can be achieved by using a gap height $h = 1$Å and a damping rate $\hbar\gamma = 400\ meV$.

It is also interesting to consider the low-energy features in the experimental data which are not well reproduced in figure 3 by the present model. Given that graphene's π electron plasmon dispersion scales as $\omega_p(q) \propto \sqrt{q}$ at long wavelengths, one may expect that it will be strongly coupled with the non-dispersing Fuchs-Kliever surface phonon mode in the SiC substrate at the frequency around $116\,meV$ [36]. Such coupling was discussed recently in reference [39] where the strong optical phonon mode in SiC was described by a simple frequency-dependent dielectric function $\varepsilon_s(\omega)$ to be used in equation (4) for the overall dielectric response of epitaxial graphene. As a result, a strong avoided crossing between the graphene's plasmon mode and the phonon mode in the substrate was predicted theoretically in reference [39] and confirmed experimentally in reference [40]. It is interesting that this plasmon-phonon coupling scenario continues to attract considerable interest [41, 42, 43].

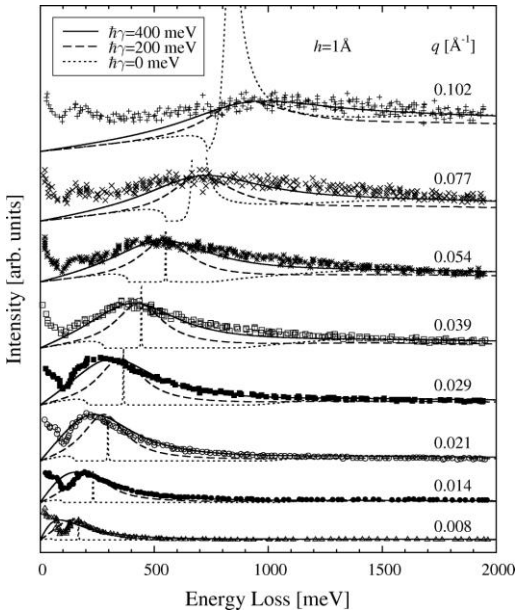

Figure 3. The Mermin loss function (in arbitrary units) versus the energy loss for graphene with a charge-carrier density $n = 2 \cdot 10^{13}\,cm^{-2}$ supported on a SiC substrate with static dielectric constant $\varepsilon_s = 9.7$ and a gap height $h = 1$ Å. Model results are shown for damping rates $\hbar\gamma = 0$, 200, and $400\,meV$, while symbols show the HREELS experimental data from reference [36].

4. Conclusions

We have presented an extensive analysis of the stopping and image forces on an external point charge moving parallel to a single layer of supported graphene under the gating conditions. Calculations of the velocity and distance dependencies of the stopping and image forces were performed within the random phase approximation (RPA) for a broad range of charge-carrier densities with two major goals: to compare the results with a semiclassical kinetic equation (KE) model, and to examine of the effects of a finite graphene-substrate gap. The third goal was to estimate a finite damping rate introduced using Mermin's procedure.

With respect to the first goal, a comparison of the forces from the RPA and KE models in the regime of vanishing damping has revealed that the latter model may be justified for particle distances satisfying $z_0 k_F > 1$ for $v < v_F$ and satisfying $z_0 k_F >> 1$ for $v > v_F$. When combined through Bohr's adiabatic criterion, these conditions suggest that the KE model is valid only for heavily doped

graphene with $E_F > \hbar v / z_0$, for which the effects of the interband single-particle excitations on the stopping and image forces are minimized. With respect to the second goal, the effects of a finite gap between graphene and a supporting substrate in the RPA model with vanishing damping have been found to be quite strong, particularly for medium to high particle speeds. These results have confirmed earlier findings from the KE model [27] and raise some concern over the common practice of treating graphene with a zero gap when dealing with the dynamic polarization forces on external moving charges. With respect to the third goal, we have made an effort to estimate the order of magnitude of the damping rate, γ, by providing a tentative fit of the RPA dielectric function modified by Mermin's procedure with experimental data for the HREELS spectra of graphene on a SiC substrate [36].

Acknowledgments
This work has been supported by the Ministry of Science and Technological Development of the Republic of Serbia (Project No. 141013). Z.L.M. acknowledges support by the Natural Sciences and Engineering Research Council of Canada. The authors are most grateful to Dr Ljupčo Hadžievski and Dr Duško Borka for many useful comments and continuing support.

References

[1] Geim A K and Novoselov K S 2007 *Nature Mater*. **6** 183
[2] Castro Neto A H, Guinea F, Peres N M R, Novoselov K S and Geim A K 2009 *Rev. Mod. Phys.* **81** 109
[3] Geim A K and Kim P 2008 *Sci. Am.* **298** 90
[4] Kramberger C, Hambach R, Giorgetti C, Rümmeli M H, Knupfer M, Fink J, Büchner B, Reining L, Einarsson E, Maruyama S, Sottile F, Hannewald K, Olevano V, Marinopoulos A G and Pichler T 2008 *Phys. Rev. Lett.* **100** 196803
[5] Eberlein T, Bangert U, Nair R R, Jones R, Gass M, Bleloch A L, Novoselov K S, Geim A K and Briddon P R 2008 *Phys. Rev.* B **77** 233406
[6] Ramos G and Scherzer B M U 1994 *Nucl. Instr. Meth.* B **85** 479
[7] Ramos G and Scherzer B M U 2001 *Nucl. Instr. Meth.* B **174** 329
[8] Yagi E, Iwata T, Urai T and Ogiwara K 2004 *J. Nucl. Mater.* **334** 9
[9] Cernusca S, Fürsatz M, Winter H P and Aumayr F 2005 *Europhys. Lett.* **70** 768
[10] Kaneko T, Kudo H, Tomita S and Uchiyama R 2006 *J. Phys. Soc. Jpn.* **75** 034717
[11] Mowbray D J, Mišković Z L, Goodman F O and Wang Y N 2004 *Phys. Rev.* B **70** 195418
[12] Mowbray D J, Mišković Z L and Goodman F O 2006 *Phys. Rev.* B **74** 195435
[13] Borka D, Petrović S, Nešković N, Mowbray D J and Mišković Z L 2006 *Phys. Rev.* A **73** 062902
[14] Borka D, Mowbray D J, Mišković Z L, Petrović S and Nešković N 2010 *New J. Phys.* **12** 043021
[15] Fetter A L 1973 *Ann. Phys*. **81** 367
[16] Stockli T, Bonard J M, Chatelain A, Wang Z L and Stadelmann P A 2001 *Phys. Rev.* B **64** 115424
[17] Borka D, Mowbray D J, Mišković Z L, Petrović S and Nešković N 2008 *Phys. Rev.* A **77** 032903
[18] Borka D, Mowbray D J, Mišković Z L, Petrović S and Nešković N 2008 *J. Phys.: Condens. Matter* **20** 474212
[19] Radović I and Borka D 2010 *Phys. Lett.* A **374** 1527
[20] Radović I, Hadžievski Lj, Bibić N and Mišković Z L 2009 *Mater. Chem. Phys*. **118** 293
[21] Radović I, Hadžievski Lj, Bibić N and Mišković Z L 2007 *Phys. Rev.* A **76** 042901
[22] Radović I and Borka D 2010 *Nucl. Instr. Meth.* B **268** 2649
[23] Pitarke J M, Silkin V M, Chulkov E V and Echenique P M 2007 *Rep. Prog. Phys.* **70** 1
[24] Wunsch B, Stauber T, Sols F and Guinea F 2006 *New J. Phys.* **8** 318
[25] Hwang E H and Das Sarma S 2007 *Phys. Rev.* B **75** 205418

[26] Barlas Y, Pereg-Barnea T, Polini M, Asgari R and Mac-Donald A H 2007 *Phys. Rev. Lett.* **98** 236601
[27] Radović I, Hadžievski Lj and Mišković Z L 2008 *Phys. Rev.* B **77** 075428
[28] Ryzhii V, Satou A and Otsuji T 2007 *J. Appl. Phys.* **101** 024509
[29] Bertoni G, Calmels L, Altibelli A and Serin V 2005 *Phys. Rev.* B **71** 075402
[30] Ishigami M, Chen J H, Cullen W G, Fuhrer M S and Williams E D 2007 *Nano Lett.* **7** 1643
[31] Prodan E, Radloff C, Halas N J and Nordlander P 2003 *Science* **302** 419
[32] Trevisanutto P E, Giorgetti C, Reining L, Ladisa M and Olevano V 2008 *Phys. Rev. Lett.* **101** 226405
[33] Mermin N D 1970 *Phys. Rev.* B **1** 2362
[34] Asgari R, Vazifeh M M, Ramezanali M R, Davoudi E and Tanatar B 2008 *Phys. Rev.* B **77** 125432
[35] Hwang E H and Das Sarma S 2008 *Phys. Rev.* B **77** 195412
[36] Liu Y, Willis R F, Emtsev K V and Seyller Th 2008 *Phys. Rev.* B **78** 201403(R)
[37] Allison K F, Borka D, Radović I, Hadžievski Lj and Mišković Z L 2009 *Phys. Rev.* B **80** 195405
[38] Pines D and Schrieffer J R 1962 *Phys. Rev.* **125** 804
[39] Allison K F and Mišković Z L 2010 *Nanotechnology* **21** 134017
[40] Liu Y and Willis R F 2010 *Phys. Rev.* B **81** 081406(R)
[41] Hwang E H, Sensarma R and Das Sarma S 2010 arXiv:1008.0862v1
[42] Tegenkamp C, Pfnür H, Langer T, Baringhaus J and Schumacher H W 2010 arXiv:1008.1013v1
[43] Koch R J, Seyller Th and Schaefer J A 2010 arXiv:1008.1130v1